Electric Double Layers with Electrolyte Mixtures: Integral Equations Theories and Simulations

A. Martín-Molina,[†] M. Quesada-Pérez,[‡] and R. Hidalgo-Álvarez*[,§]

Laboratoire de Physique Statistique de l'Ecole Normale Supérieure associée au CNRS, Universités Paris VI et Paris VII, 24 rue Lhomond, 75231 Paris Cedex 05, France, Departamento de Física, Universidad de Jaén, Escuela Universitaria Politécnica, 23700 Linares, Jaén, Spain, and Grupo de Física de Fluidos y Biocoloides, Departamento de Física Aplicada, Facultad de Ciencias, Universidad de Granada, 18071 Granada, Spain

Received: July 19, 2005

A study of a planar electric double layer (EDL) in the presence of mixtures of electrolyte is presented. In particular, results from the Hyper-Netted-Chain/Mean-Spherical-Approximation (HNC/MSA) theory are compared with Monte Carlo (MC) simulations. In this way, the charge inversion induced by mixtures of multivalent and monovalent counterions is probed. Since overcharging phenomena in nature emerge under such conditions, the role of ion−ion correlations in the EDL appears as a crucial point in this kind of study. Unlike previous related works, a realistic hydrated ion size is used in the HNC/MSA calculations and simulations. In this way, a qualitative agreement between the results obtained from the theory and MC simulations is found. However, some discrepancies arise when the charge inversion is expected to be more noticeable, namely at high surface charges and/or elevated concentrations of multivalent electrolytes. Such differences are explained in terms of an overestimation of the charge inversion by the integral equation (IE) formalism.

I. Introduction

In the last several years there has been a resurgent interest in the study of the EDL. Since colloidal dispersions are often electrostatically stabilized, the structure of the electrolyte near a charged surface has practical relevance in many areas of technology and also in biological systems. Although the classical Gouy−Chapman (GC) theory of EDL is satisfactorily applied to systems where the concentration of (mostly monovalent) electrolyte and the surface charge are low enough, this model fails under certain conditions. For instance, errors in the GC theory are noticeable for multivalent electrolytes, for elevated monovalent salt concentrations, for ions with a large diameter, for high surface charges, and for solvents with a lower dielectric coefficient. These errors have been previously corroborated by comparing the classical theory with a large variety of simulations and sophisticated models such as the modified Poisson−Boltzmann (MPB) theory, the density functional theory (DFT), and those models based on integral equations (IE) theories.[1−10] Moreover, computer simulation appears as a powerful tool to test the validity of the theoretical formalisms cited above. However, the largest ionic diameters used in these works have always been 0.425 nm. This value is considerably smaller than the hydrated ion size found in the scientific literature (even for monovalent ions).[11−13] Here, one can find diameters of many ions of diverse valences obtained from X-ray and neutron diffraction studies on solids and from gas solubility, viscosity, and self-diffusion on liquids as well as from thermodynamics studies of ion solvation. Apart from that, the consideration of hydrated ions (instead of the bare ones) is well established in the double layer theory. For instance, the Outer Helmholtz Plane is located just at a distance equal to the hydrated ion radius from the macroparticle surface.[14]

The relevance of the realistic hydrated ion size has already been studied by MC simulations in a preceding survey.[15] According to this work, the HNC/MSA overestimates the charge reversal effects when the ion diameter is larger than 0.425 nm.

Furthermore, despite the spectacular increase in the number of studies dealing with EDLs performed since the early 80s, the presence of mixtures of electrolytes has been scarcely addressed.[16−21] However, phenomena such as the DNA condensation are induced by the addition of multivalent electrolytes to a solution at physiological conditions (0.1 M of NaCl).[22] Therefore, a study of EDLs in solutions comprised of counterions with dissimilar valences and realistic sizes appears as an important issue toward the better understanding of this type of phenomena. In this sense, to our knowledge, an explicit comparison between results from IE theories and simulations for electrolyte mixtures has not been reported so far. In particular, we will focus on mixtures of 3:1 and 1:1 salts since charge inversion takes place clearly in the presence of trivalent or highly charged counterions.

II. HNC/MSA Equations for a Multicomponent System

In this work, we have used a representation of the EDL based on the primitive model. Accordingly, small ions are treated as charged hard spheres immersed in a dielectric continuum. The Ornstein−Zernike (OZ) formalism (applied to isotropic system) can be the starting point in the description of such EDL:

$$h_{ik}(r) = c_{ik}(r) + \sum_{j=0}^{4} \rho_j \int c_{ij}(|\vec{r} - \vec{s}|) h_{jk}(s)\, \mathrm{d}^3 s \qquad (1)$$

* Address correspondence to this author. Phone: (+34) 958-243-213. Fax: (+34) 958-243-214. E-mail: rhidalgo@ugr.es.
[†] Universités Paris VI et Paris VII.
[‡] Escuela Universitaria Politécnica.
[§] Universidad de Granada.

10.1021/jp053970n CCC: $33.50
Published on Web 12/24/2005

where $h_{ik}(r)$ is the total correlation function of species i and k (by definition, $h_{ik}(r) \equiv g_{ik}(r) - 1$, where $g_{ik}(r)$ is the radial distribution function), ρ_j is the density of species j, and $c_{ik}(r)$ are the so-called *direct* correlation functions (also for species i and k). As we are interested in the case of a mixture of two electrolytes (3:1 and 1:1), there will be four different types of ions. The indexes i, j, and k run from 0 to 4, where 0 refers to colloidal particles (macroions), 1 and 3 refer to counterions of the electrolytes 3:1 and 1:1, respectively, and finally indexes 2 and 4 will be used for the co-ions associated with the salts 3:1 and 1:1, respectively. If we restrict ourselves to the case of highly dilute suspensions ($\rho_0 \rightarrow 0$), the OZ equation for ion−particle correlations can be written as:

$$h_{i0}(r) = c_{i0}(r) + \sum_{j=1}^{4} \rho_j \int c_{ij}(|\vec{r} - \vec{s}|) h_{j0}(s)\, \mathrm{d}^3 s \qquad (2)$$

The next steps can be summarized as follows. First, the particle−ion direct correlation function ($c_{i0}(r)$) is expressed in terms of $h_{i0}(r)$ with the help of the HNC equation whereas the ion−ion direct correlation functions are treated with the MSA. After performing certain algebraic manipulations, angular integrations, and the reduction to the case of a *planar* surface (see refs 23−25 for further details), the HNC/MSA equations for this multicomponent system (in the presence of a planar charge surface) turn out to be:

$$\ln[g_{i0}(r)] = -\beta Z_i e \psi(r) + \sum_{j=1}^{4} \rho_j \int_{-\infty}^{+\infty} C_{ij}^{0}(|x - y|) h_{j0}(y)\, \mathrm{d}y \qquad (3)$$

where $\beta = 1/k_B T$ (k_B is Boltzmann's constant and T is the absolute temperature), Z_i is the valence of species i, e is the elementary charge, $\psi(r)$ is the electrostatic potential, and $C_{ij}^{0}(|x - y|)$ are *integrals* depending on the *direct* correlation functions of the bulk species (calculated from ref 24).

III. Monte Carlo Simulations

In this section we present the details of the MC simulation performed for the description of the planar EDL based on a primitive model of electrolyte. The plane wall is assumed to be smooth and uniformly charged. The calculations have been carried out by using the Metropolis algorithm applied to a canonical ensemble for a collection of N ions confined in a rectangular prism (or cell) of dimensions $W \times W \times L$. The impenetrable charged wall is located at $z = 0$ whereas at $z = L$ another impenetrable wall without charge is placed. Accordingly, periodic boundary conditions were used in the lateral directions (x and y). The cell contains the ionic mixture corresponding to the bulk electrolyte solution together with an excess of counterions neutralizing the surface charge. The interaction energy between mobile ions is given by

$$u(\vec{r}_{ij}) = \frac{Z_i Z_j e^2}{4\pi\epsilon_0 \epsilon_r r_{ij}} \qquad \text{for } r_{ij} > d$$

$$u(\vec{r}_{ij}) = \infty \qquad \text{for } r_{ij} < d \qquad (4)$$

where d is the hydrated ion diameter, $\epsilon_r\epsilon_0$ are the relative permittivity of the dielectric continuum and the vacuum, respectively, $\vec{r}_{ij}$ is the relative position vector, and $r_{ij} = |\vec{r}_{ij}|$ is the distance between ions i and j, whereas the interaction energy of ion i with the charged wall is

$$u(\vec{r}_i) = \frac{\sigma_0 Z_i e z_i}{2\epsilon_0 \epsilon_r} \qquad (5)$$

where z_i is the z-coordinate of particle i, and σ_0 is the surface charge density of the charged wall.

The number of ions in each simulation was fixed, checking that the cell size was always large enough. Likewise, the systems were always thermalized before collecting data for averaging and the acceptance ratio was kept between 0.4 and 0.6.

Due to the long range of the electrostatic interactions, the energy must be evaluated very carefully. In these simulations, we have applied the so-called *external potential method* (EPM), in which each mobile ion is allowed to interact with the others in the MC cell according to the usual minimum image convention.[1−3,26] The remaining part (all charges outside the cell) is considered in the evaluation energy through an external potential, $\psi_{ext}(z)$. This function is calculated assuming that the ionic distribution profiles outside the cell are identical with those inside. Thus the external potential must be updated during the simulation by using the current ion profiles and is given by

$$\psi_{ext}(z) = \frac{1}{4\pi\epsilon_0\epsilon_r} \int_0^L \int_{\pm W/2}^{\pm\infty} \int_{\pm W/2}^{\pm\infty} \frac{\rho(z')}{\sqrt{(x')^2 + (y')^2 + (z' - z)^2}}\, \mathrm{d}x'\, \mathrm{d}y'\, \mathrm{d}z' \qquad (6)$$

where $\rho(z')$ is the charge density at z' (both outside and inside the cell). The integration over x' and y' can be performed analytically, whereas the integration over z' must be carried out numerically since the function $\rho(z')$ is tabulated. This is equivalent to considering the electrostatic potential generated by a set of infinite sheets of thickness $\mathrm{d}z'$ and surface charge density $\rho(z')\, \mathrm{d}z'$ from which the central square "hole" (of dimensions $W \times W$) is removed. The electrostatic potential of an *entire* infinite sheet can be calculated as in eq 5, whereas the electrostatic potential of the square hole removed from its center, which must be subtracted, can be calculated by using the integral appearing in eq 16 of ref 26. In a previous work,[15] the energy was also calculated by following an alternative method to the EPM, originally developed by Lekner for systems with 2D symmetries, that has recently been improved by Sperb.[27,28] However, no significant differences were found in comparing with the EPM.

Having computed the local ion concentrations, the diffuse potential can be calculated from

$$\psi_d \equiv \psi(a) = \frac{e}{\epsilon_r \epsilon_0} \int_a^{\infty} (a - z) \sum_j Z_j \rho_j(z)\, \mathrm{d}z \qquad (7)$$

where $a = d/2$ is the hydrated ion radius and $\rho_j(z)$ is the local density of j-ions at a distance z from the charged surface ($j = 1, 2, 3$ for trivalent counterions, monovalent counterions, and co-ions, respectively). The integral appearing in eq 7 should be evaluated over an infinite interval, but this is not feasible in practice because computer simulations are always carried out in a box with a finite length (L). To take this aspect into account, it is usual to choose a cutoff distance (L_c) admitting that, theoretically, the contribution to such an integral is negligible (for $z > L_c$) if $\sum_{j=1,2} Z_j \rho_j(z) = 0$. This is the condition of local electroneutrality, which can always be fulfilled far enough from the charged surface (in the solution bulk). Due to the term ($a - z$), however, the fluctuations of $\sum_{j=1,2} Z_j \rho_j(z)$ (computed from simulations) could be considerably amplified, contributing

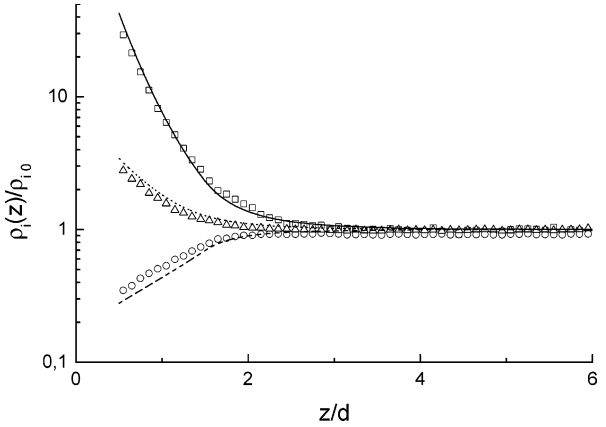

Figure 1. Local *i*-ion concentration (normalized by the bulk value) as a function of the distance from the charged surface (normalized by the ion diameter) for $d = 90$ nm, $\sigma_0 = -0.04$ C/m^2, $C_{3:1} = 10$ mM, and $C_{1:1} = 50$ mM. Squares, triangles, and circles stand for MC simulations for trivalent counterions, monovalent counterions, and co-ions, respectively. Solid, dotted, and dashed lines represent HNC/MSA predictions for trivalent counterions, monovalent counterions, and co-ions, respectively.

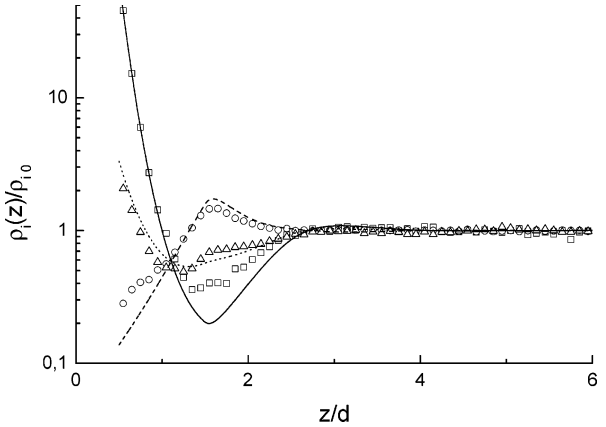

Figure 2. Local *i*-ion concentration as a function of the distance from the charged surface for $d = 90$ nm, $\sigma_0 = -0.16$ C/m^2, $C_{3:1} = 100$ mM, and $C_{1:1} = 100$ mM. Symbols and lines mean the same as in Figure 1.

appreciably to the integral of eq 7. To avoid this undesirable contribution L_c must not be too large. In our runs, we took $L_c = 0.5L$, and chose values for L trying to guarantee the electroneutrality condition at $0.5L$. The diffuse potential and its statistical error were computed by collecting many averages of ψ_d (according to eq 7) during the runs.

IV. Results and Discussion

As mentioned before, the main objective of this work is a comparison of simulation data and those obtained from the IE theories in the study of planar EDLs with mixtures of tri- and monovalent counterions (the corresponding salt concentrations are $C_{3:1}$ and $C_{1:1}$, respectively). To this end, the present section is organized as follows: First, the theoretical distribution curves of ions are compared with those obtained via simulations for three illustrative cases and the occurrence of the charge inversion is discussed. Second, the effect of the surface charge density is analyzed. Then, the effect of the salt concentrations in the mixture is also studied by using both numerical techniques. Finally, the importance of the ion size is probed.

(a) Ionic Profiles. In Figures 1−3 the local ion concentrations, ρ_i, normalized by the concentration at the bulk solution, ρ_{i0}, are shown as a function of the distance from the surface (z)

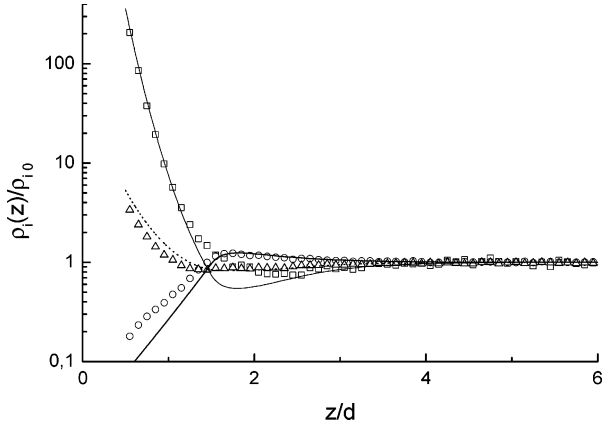

Figure 3. Local *i*-ion concentration as a function the distance from the charged surface for $d = 90$ nm, $\sigma_0 = -0.115$ C/m^2, $C_{3:1} = 10$ mM, and $C_{1:1} = 100$ mM. Symbols and lines mean the same as in Figure 1.

under three different conditions, respectively. Let us start with a case in which charge inversion is not expected to take place, that is, small surface charge density and low ionic concentrations. Such a situation is presented in Figure 1 where the ionic profiles are plotted for a planar EDL with $\sigma_0 = -0.04$ C/m^2, $C_{3:1} = 10$ mM, and $C_{1:1} = 50$ mM. As can be seen, all the ionic profiles are monotonic and a good agreement between theory and simulations is observed. More specifically, these functions are increasing for co-ions and decreasing for trivalent and monovalent counterions. This monotonic behavior is characteristic of systems in which the classical theory of EDL can reproduce the results properly and thus more sophisticated models are not required, a priori, to describe the systems. However, what happens when the surface charge and electrolyte concentrations increase? This situation is examined in Figure 2 where the ionic distributions are shown for $\sigma_0 = -0.16$ C/m^2, $C_{3:1} = 100$ mM, and $C_{1:1} = 100$ mM. These curves strongly contrast with the previous ones since they are not monotonic any longer. This feature cannot be explained in terms of the classical GC theory, which always predicts monotonic profiles. In Figure 2, the counterion distribution curves obtained from the HNC/MSA and simulations exhibit a minimum near the surface whereas the co-ion distribution presents a maximum at the same location. From this position, the co-ion concentration decreases and the counterion concentrations increase, just if the surface charge had the opposite sign and their respective roles were inverted. This behavior suggests the existence of charge inversion. Although both theory and simulations are able to capture the oscillations, these are more pronounced for the HNC/MSA case. It means that IE theory overestimates the hallmarks of charge inversion under these conditions. Indeed, differences between the ion distribution functions predicted by the HNC/MSA and the simulations for only one type of electrolyte (3:1) have been reported in a previous paper.[15]

Finally, Figure 3 illustrates a crossover situation between the preceding ones for $\sigma_0 = -0.115$ C/m^2, $C_{3:1} = 10$ mM, and $C_{1:1} = 100$ mM. The ionic distribution functions are not monotonic but the oscillating behavior has not become very pronounced yet.

(b) Surface Charge Effect. To study the surface charge effect in the occurrence of charge inversion, the diffuse potential has been calculated as a function of σ_0 for several conditions. The diffuse potential is a key property in colloid science. In particular, it is intimately related to the ζ-potential, an essential quantity to characterize and analyze electrokinetic phenomena. To begin with, we examine in Figure 4 the appearance of diffuse potential reversals with increasing the magnitude of σ_0 for two

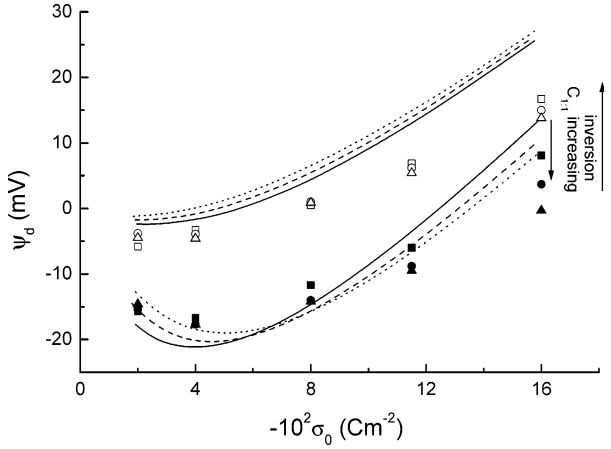

Figure 4. Diffuse potential as a function of the surface charge density for $d = 90$ nm. Solid and open symbols represent MC simulations for $C_{3:1} = 10$ and 100 mM, respectively. Squares, circles, and triangles denote $C_{1:1} = 0$, 50, and 100 mM, respectively. Solid, dotted, and dashed lines represent HNC/MSA predictions for $C_{1:1} = 0$, 50, and 100 mM, in that order ($C_{3:1} = 10$ and 100 mM upper and lower curves, respectively).

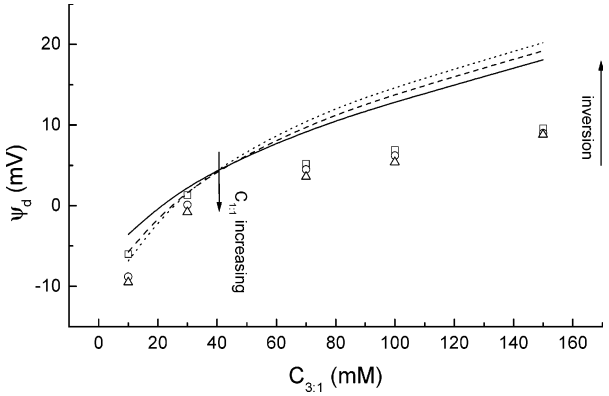

Figure 5. Diffuse potential as a function of the concentration of 3:1 electrolyte for $d = 90$ nm and $\sigma_0 = -0.115$ C/m^2. Squares, circles, and triangles denote MC simulations for $C_{1:1} = 0$, 50, and 100 mM, respectively. Solid, dotted, and dashed lines represent HNC/MSA predictions for $C_{1:1} = 0$, 50, and 100 mM, in that order.

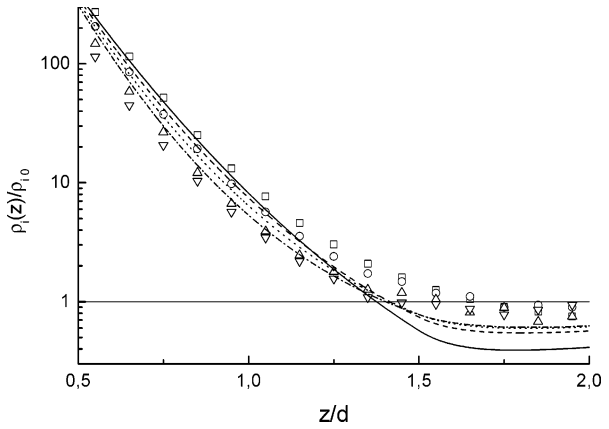

Figure 6. Local trivalent ion concentration (normalized by the bulk value) as a function the distance from the charged surface (normalized by the ion diameter) for $d = 0.90$ nm, $\sigma_0 = -0.115$ C/m^2, and $C_{3:1} = 10$ mM. $C_{1:1} = 0$ (squares and solid line), 100 (circles and dashed line), 200 (up triangles and dotted line), and 300 (down triangles and dashed−dotted line). Symbols and lines denote MC simulations and HNC/MSA predictions, respectively.

3:1 electrolyte concentrations (10 and 100 mM) and three monovalent salt concentrations (0, 50, and 100 mM). In general, the agreement between MC simulations and the HNCMSA results is significant. According to both treatments, the presence of trivalent counterions has a clear influence on ψ_d. With increasing $C_{3:1}$ from 10 to 100 mM the $\psi_d-\sigma_0$ plots shift toward the region of reversals noticeably. Simultaneously, the inversion surface charge density, that is, the σ_0 value at which the reversal appears, decreases considerably. In contrast, the effect of the monovalent salt is not so marked. In the case of $C_{3:1} = 10$, the effect of the 1:1 electrolyte in the potential is different depending on the surface charge value. More specifically, an increase of $C_{1:1}$ for $\sigma_0 < 0.06$ C m^{-2} implies a slight reduction in the absolute value of the diffuse potential. On the contrary, the curves shift toward more negative values for $\sigma_0 > 0.06$ C m^{-2}. Here, an increase of the monovalent salt reduces the potential inversion. Concerning the results for $C_{3:1} = 100$ mM, the effect of the monovalent salt is almost negligible. In particular, the simulations data are practically the same for the three cases, whereas slight differences can be found in the HNCMSA curves. At any rate, the effect of each ionic species in the mixture is specifically studied in the following section.

(c) Effect of Multi- and Monovalent Ions. In Figure 5, the diffuse potential is plotted vs the concentration of asymmetric (3:1) electrolyte for $C_{1:1} = 0$, 50, and 100 mM. As can be seen, the theoretical results reproduce the simulation data, at least qualitatively. For instance, a potential reversal due to trivalent counterions is reached for values of $C_{3:1}$ between 20 and 40 mM. Both techniques agree in the fact that these reversal concentrations tend to shift slightly toward larger values as $C_{1:1}$ increases. This feature has also been reported in previous electrokinetic experiments.[25] Likewise, for negative diffuse potentials, theory and simulations similarly show that a rise in the monovalent salt concentration involves an increase in magnitude of ψ_d. Although this behavior is not intuitive from a classical point of view, different authors have experimentally observed it.[25,30]

Once the sign of the potential is inverted, some discrepancies appear between the HNC/MSA and the MC simulation. The later points toward the existence of a saturation value for ψ_d whereas the former predicts an increase in the magnitude of the inverted potential, at least for the range of multivalent salt concentrations employed in this work. The existence of a saturation value in the diffuse potential can be inferred from the electrophoretic mobility experiments for a sulfonate latex performed by Martín-Molina et al.[25] Furthermore, if one admits that the well-known Helmholtz−Smoluchowski approximation is valid in this case (high values for κa_0, where κ is the Debye screening parameter and a_0 the macroparticle radius), ψ_d can be readily converted into μ_e. As a result, the saturation value of electrophoretic mobility so obtained turns out to be about 0.4 $\times 10^{-8}$ m^2/(V·s), practically equal to that found experimentally for the sulfonate latex.[25] In addition, slight differences can be also found in the effect of the monovalent salt at the saturation regime. Here, the HNCMSA predicts a decrease of ψ_d with $C_{1:1}$ whereas such an effect is not observed by the simulation curves, which tend to converge to similar values as the presence of trivalent ions becomes more noticeable. As a consequence, a failure of the approximations of the IE formalism is likely to be happening under these conditions.

To deepen into the role of monovalent ions in the electrolyte mixture at low and high multivalent salt concentrations, we have analyzed the effect of $C_{1:1}$ on the distribution profiles of trivalent ions for short distances (close to the charged surface) and $\sigma_0 = -0.115$ C/m^2. Accordingly, Figure 6 deals with the case of noninversion ($C_{3:1} = 10$mM) by means of IE equations a MC simulations. As can be observed in both cases, the monovalent

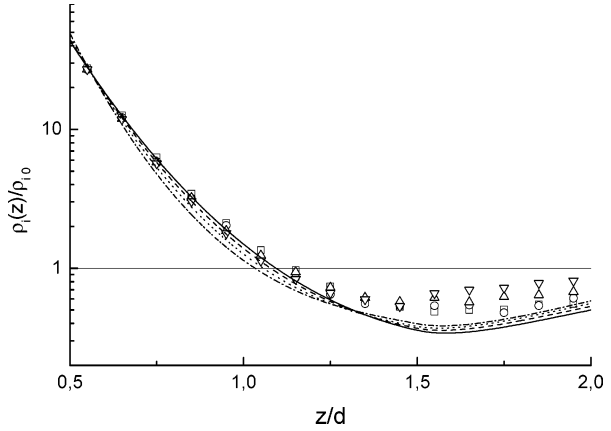

Figure 7. Local trivalent ion concentration (normalized by the bulk value) as a function the distance from the charged surface (normalized by the ion diameter) for $d = 0.90$ nm, $\sigma_0 = -0.115$ C/m^2, and $C_{3:1} = 100$ mM.. Symbols and lines mean the same as in Figure 6.

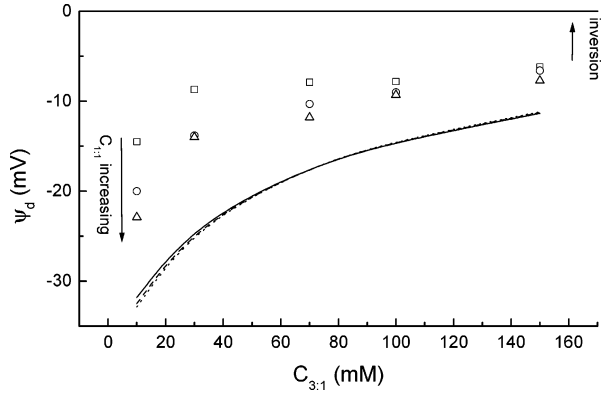

Figure 8. Diffuse potential as a function of the concentration of 3:1 electrolyte for $d = 0.40$ nm and $\sigma_0 = -0.115$ C/m^2. Symbols and lines mean the same as in Figure 5.

counterions tend to displace the trivalent ones as $C_{1:1}$ becomes larger. The case of high concentrations of the trivalent salt, $C_{3:1} = 100$ mM, is studied in Figure 7. Unlike the preceding case, the addition of monovalent salt does not seem to have an important influence on the trivalent ion distribution. This is rather reasonable since the number of trivalent ions is comparable to that of monovalent ions.

Apart from that, a minimum in the distribution curves at distances around 1.5*d* is manifest according to the theory and simulations. However, some differences between both approaches are found. In particular, the IE formalism predicts a larger magnitude of the minimum. Since the minimum appears as a consequence of the high counterion concentrations in the immediate vicinity of the charged surface, these differences point out that the HNC/MSA is probably overestimating the accumulation of counterions in the neighborhood of the charged surface.[15]

(d) Effect of Ion Size. With the aim of probing the effects of the ionic excluded volume as the driving force of overcharging in the system studied here, we have explored ion sizes smaller than those employed to obtain Figure 5. In particular, we simulated $\psi_d - C_{3:1}$ curves by using a diameter of 0.4 nm for all ionic species. As we mentioned before, this value is quite similar to that used in most previous studies of EDLs. The results are shown in Figure 8. As can be seen, the shift of the curves toward the no-inversion regime upon addition of 1:1 electrolyte is also observed. However, the most outstanding feature of this figure is that the inversion has disappeared, which clearly proves that the value of the ionic diameters is not a trivial matter. In

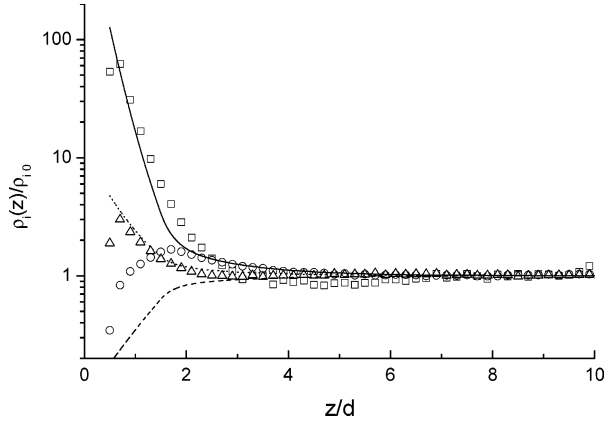

Figure 9. Local *i*-ion concentration as a function of the distance from the charged surface for $d = 0.40$ nm, $\sigma_0 = -0.115$ C/m^2, $C_{3:1} = 30$ mM, and $C_{1:1} = 50$ mM. Symbols and lines mean the same as in Figure 1.

this manner, the hydrated ion sizes extracted from the scientific literature appear to be an adequate choice. Moreover, the disappearance of overcharging in reducing the ion size has also been reported by other authors.[31] Likewise, although the HNC/MSA data confirm the disappearance of the inversion, quantitative differences can be observed in relation to the simulations. Furthermore, the effect of the monovalent salt appears irrelevant. To explain this feature, the distribution functions for $\sigma_0 = -0.115$ C/m^2, $C_{3:1} = 30$ mM, $C_{1:1} = 50$ mM, and $d = 0.40$ nm are plotted in Figure 9. As can be observed, the simulations predict a maximum in the co-ion distribution curve, which is not predicted by the HNC/MSA. This accumulation of the co-ions near the charged surface could appear as a consequence of the electrostatic attraction between multivalent counterions and co-ions (stronger for smaller ions). In this way, the multivalent counterions moving toward the surface would drag an important quantity of co-ions with them. Probably, this effect is not predicted by the IE theory whose validity is reduced as the ion size becomes smaller.

V. Conclusions

In general, the results indicate that the charge inversion of EDLs with electrolyte mixtures can be described fairly well by using IE theories and MC simulations. However, some discrepancies have been observed. An overestimation of charge reversal effects is probably responsible for the numerical differences. Despite this quantitative disagreement, it has been proved that ion size correlations play a fundamental role in charge inversion, in agreement to other works that apply different techniques and/or theoretical approaches.[9,13,15,25,31−34] Indeed, it has been proved that the charge inversion depends on the ionic size chosen in the calculations. Moreover, the use of the traditional ion sizes (0.4 nm) instead of the realistic ones involves the disappearance of the charge inversion in colloidal systems under real conditions. Apart from that, such reduction in the ion size gives rise to quantitative differences between IE theories and simulations. Nevertheless, it must be taken into account that the primitive model used here is too rudimentary to rationalize the behavior of all real colloids. For instance, the only interaction considered between small ions and the particle surface is given by eq 5. Therefore, more complex interactions between the charged surface and the ions (for instance, those depending on their chemical nature) are required for a complete description of phenomena such as charge inversion. In fact, mobility reversals in the presence of extremely low concentrations of 3:1 elec-

trolytes (of about 10^{-5} M) have been observed for carboxylic latexes,[35] liposomes,[36] retroviruses,[37] and unicellular algae.[38] In all these cases, the hypothesis of a specific adsorption of ions on the surface due to interactions not considered in this work could be reasonable, since simulations and integral equation theories predict much larger inversion concentrations. At any rate, the inclusion of the ion size correlations is found to always entail an improvement in the description of the EDL, in relation to those models that neglect the ionic size.

Acknowledgment. M.Q.-P. and R.H.-A. are grateful to "Ministerio de Ciencia y Tecnología, Plan Nacional de Investigación, Desarrollo e Innovación Tecnológica (I+D+I)" for financial support, project nos. MAT2003-08356-C04-01 and MAT2003-01257, respectively. A.M.-M. thanks the postdoctoral contract from the "Ayudas para el Perfeccionamiento de Investigadores de la Junta de Andalucía". The authors also wish to acknowledge the contribution of J. Maldonado-Valderrama.

References and Notes

(1) van Megen, W.; Snook, I. *J. Chem. Phys*. **1980**, *73*, 4656.
(2) Torrie, G. M.; Valleau, J. P. *J. Chem. Phys.* **1981**, *73*, 5807.
(3) Torrie, G. M.; Valleau, J. P. *J. Phys. Chem.* **1982**, *86*, 3251.
(4) Mier-y-Teran, L.; Suh, S. H.; White, H. S.; Davis, H. T. *J. Chem. Phys.* **1990**, *92*, 5087.
(5) Degrève, L.; Lozada-Cassou, M.; Sánchez, E.; González-Tovar, E. *J. Chem. Phys.* **1993**, *98*, 8905.
(6) Degrève, L.; Lozada-Cassou, M. *Mol. Phys.* **1995**, *86*, 759.
(7) Boda, D.; Fawcett, W. R.; Henderson, D.; Sokolowski, S. *J. Chem. Phys.* **2002**, *116*, 7170.
(8) Bhuiyan, B.; Outhwaite, C. W. *Phys. Chem. Chem. Phys.* **2004**, *6*, 3467.
(9) Valiskó, M.; Henderson, D.; Boda, D. *J. Phys. Chem. B* **2004**, *108*, 16548.
(10) Henderson, D.; Gillespie, D.; Nagy, T.; Boda, D. *J. Chem. Phys.* **2005**, *122*, 084504.
(11) Marcus, Y. *Ion Solvation*; John Wiley and Sons: Chichester, UK, 1985.
(12) Israelachvili, J. *Intermolecular And Surface Forces*, 2nd ed.; Academic Press: London, UK, 1992.
(13) Besteman, K.; Zevenbergen, M. A. G.; Heering, H. A.; Lemay, S. G. *Phys. Rev. Lett.* **2004**, *17*, 170802.
(14) Elimelech, M.; Gregory, J.; Jia, X.; Williams, R. *Particle Deposition & Aggregation. Measurement, Modelling and Simulation*; Butterwoth Heinemann: Amsterdam, The Netherlands, 1995.
(15) Quesada-Pérez, M.; Martín-Molina, A.; Hidalgo-Álvarez, R. *J. Chem. Phys.* **2004**, *121*, 8618.
(16) Mukherjee, A. K.; Schmitz, K. S.; Bhuiyan, L. B. *Langmuir* **2004**, *20*, 11802.
(17) Deserno, M.; Jiménez-Ángeles, F.; Holm, C.; Lozada-Cassou, M. *J. Phys. Chem. B* **2001**, *44*, 10983.
(18) Boda, D.; Varga, T.; Henderson, D.; Busath, D. D.; Nonner, W.; Gillespie, D.; Eisenberg, B. *Mol. Simul.* **2004**, *30*, 89.
(19) Delville, A.; Gasmi, N.; Pellenq, R. J. M.; Caillol, J. M.; Van Damme, H. *Langmuir* **1998**, *14*, 5077.
(20) Diehl, A.; Levin, Y. *J. Chem. Phys.* **2004**, *121*, 12100.
(21) Lobaskin, V.; Qamhieh, K. *J. Phys. Chem. B* **2003**, *107*, 8022.
(22) Gelbart, W. M.; Bruinsma, R. F.; Pincus, P. A.; Parsegian, V. A. *Phys. Today* **2000**, *53*, 38.
(23) Lozada-Cassou, M.; Saavedra-Barrera, R.; Henderson, D. *J. Chem. Phys.* **1982**, *77*, 5150.
(24) González-Tovar, E.; Lozada-Cassou, M. *J. Phys. Chem.* **1989**, *93*, 3761.
(25) Martín-Molina, A.; Quesada-Pérez, M.; Galisteo-González, F.; Hidalgo-Álvarez, R. *J. Phys.*: *Condens. Matter* **2003**, *15*, S3475.
(26) Jonson, B.; Wennerström, H.; Halle, B. *J. Phys. Chem.* **1980**, *84*, 2179.
(27) Lekner, J. *Phys. A* **1991**, *176*, 485.
(28) Sperb, R. *Mol. Simul.* **1998**, *20*, 179.
(29) Moreira, A. G.; Netz, R. R. *Eur. Phys. J. E* **2002**, *8*, 33.
(30) Elimelech, M.; O'Melia, C. R. *Colloid Surf.* **1990**, *44*, 165.
(31) Messina, R.; González-Tovar, E.; Lozada-Cassou, M.; Holm, C. *Europhys. Lett.* **2002**, *60*, 383.
(32) Quesada-Pérez, M.; González-Tovar, E.; Martín-Molina, A.; Lozada-Cassou, M.; Hidalgo-Álvarez, R. *ChemPhysChem* **2003**, *4*, 234.
(33) Martín-Molina, A.; Quesada-Pérez, M.; Galisteo-González, F.; Hidalgo-Álvarez, R. *J. Chem. Phys.* **2003**, *118*, 4183.
(34) Ravindran, S.; Wu, J. *Langmuir* **2004**, *20*, 7333.
(35) Ottewill, R. H.; Shaw, J. N. *J. Colloid Interface Sci.* **1968**, *26*, 110.
(36) Verbich, S. V.; Dukhin, S. S.; Matsumura, H. *J. Dispersion Sci. Technol.* **1999**, *20*, 83.
(37) Taylor, D. H.; Bosmann, H. B. *J. Colloid Interface Sci.* **1981**, *83*, 153.
(38) Gimmler, H.; Schieder, M.; Kowalski, M.; Zimmermann, U.; Pick, U. *Plant Cell Environ.* **1991**, *14*, 261.